

Easily Accessible Protein Nanostructures via Enzyme Mediated Addressing

Arne A. Rüdiger,[†] Katharina Brassat,^{‡,§} Jörg K. N. Lindner,^{‡,§} Wolfgang Bremser,^{||} and Oliver I. Strube^{*,†,ⓑ}

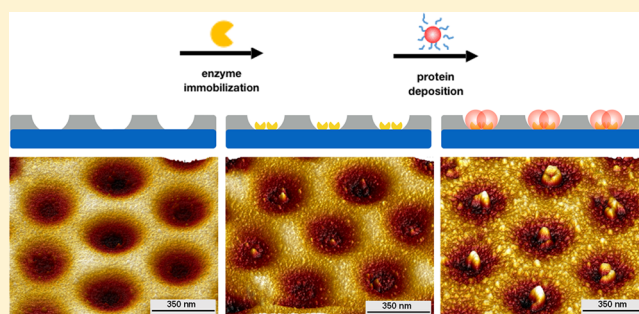
[†]Paderborn University, Department of Chemistry—Biobased and Bioinspired Materials, Warburger Str. 100, D-33098 Paderborn, Germany

[‡]Paderborn University, Department of Physics—Nanostructuring, Nanoanalysis, and Photonic Materials, Warburger Str. 100, D-33098 Paderborn, Germany

[§]Center for Optoelectronics and Photonics Paderborn (CeOPP), Warburger Str. 100, D-33098 Paderborn, Germany

^{||}Paderborn University, Department of Chemistry—Coatings, Materials and Polymers, Warburger Str. 100, D-33098 Paderborn, Germany

ABSTRACT: Site-specific formation of nanoscaled protein structures is a challenging task. Most known structuring methods are either complex and hardly upscalable or do not apply to biological matter at all. The presented combination of enzyme mediated autodeposition and nanosphere lithography provides an easy-to-apply approach for the buildup of protein nanostructures over a large scale. The key factor is the tethering of enzyme to the support in designated areas. Those areas are provided via pre patterning of enzymatically active antidots with variable diameters. Enzymatically triggered protein addressing occurs exclusively at the intended areas and continues until the entire active area is coated. After this, the reaction self-terminates. The major advantage of the presented method lies in its easy applicability and upscalability. Large-area structuring of entire support surfaces with features on the nanometer scale is performed efficiently and without the necessity of harsh conditions. These are valuable premises for large-scale applications with potentials in biosensor technology, nanoelectronics, and life sciences.



INTRODUCTION

Nanostructures from Biological Polymers. Structured surfaces and coatings based on biological polymers are highly promising materials for manifold applications with regard to biocompatibility, biodegradability, sustainability, nontoxicity, and biofunctionality.^{1–5}

While films and microstructures are easily accessible by manifold methods, structuring of surfaces with biomolecules on the sub-micrometer and nanometer scale is difficult to achieve. Frequently used methods for inorganic materials or synthetic polymers, such as lithography or etching techniques, mostly fail. This is because biopolymers are much more sensitive toward the commonly applied conditions in these processes. Especially proteins are sensitive to denaturation via thermal or mechanical stress, or exposure to irradiation and organic solvents.

Though high precision structuring with such materials, even on the lower nanometer scale, is achievable by scanning probe techniques,^{6–8} its real-world application is hindered by severe drawbacks. The applied techniques are highly time, money, and energy consuming. Another approach is the combination of photolithography and biological self-assembly to obtain well-defined biological structures with complex geometries on the nanometer scale.^{9–11} However, the respective techniques are mostly applicable to only a limited variety of biomolecules, and

deposition of these structures onto surfaces results in arbitrary patterns. Moreover, all of these current approaches inherit essential issues, if structuring of larger surfaces or higher amounts, essential for any industrial application, is considered.

An interesting alternative is the use of enzymes as a mediating agent to obtain structured surfaces with biomolecules and a high level of control, as most enzymes exhibit diameters of only a few nanometers and operate on the angstrom level. Their potential for nanostructuring has already been proven in combination with scanning probe techniques.¹² However, again, these techniques are highly complex and hardly upscalable. In principle, though, enzymes are very promising candidates for the intended purpose of biomolecule nanostructuring. In addition to their specific catalyzing properties, they exhibit further beneficial attributes toward an environmentally friendly process. They are nontoxic, sustainable, and work under mild and energy efficient conditions.

In summary, a structuring method that takes advantage of the specific enzyme properties, while being independent of

Received: November 29, 2017

Revised: March 2, 2018

Published: March 26, 2018

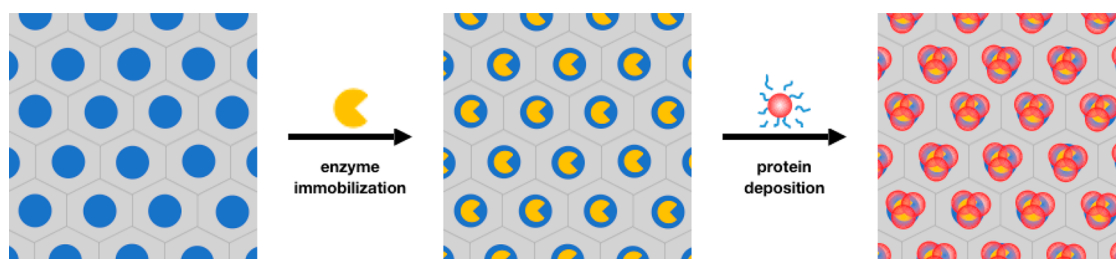


Figure 1. Approach for site-specific deposition of single protein particles via enzyme mediated autodeposition with use of a prepatterned support, obtained by nanosphere lithography. Both steps are performed as hassle-free dip-coating processes.

complex methodology, is highly desirable to enable controlled and upscalable nanostructures of biopolymers.

Nanostructuring via Enzyme Mediated Autodeposition. In this study, we introduce an easy-to-apply method for site-specific deposition of single biological particles, enabling structuring of surfaces on the nanometer scale. The approach is based on our original concept of enzyme mediated autodeposition (EMA).^{13–17} This technique combines industrially relevant and easy-to-apply autodeposition methods with the selectivity and specificity of enzymes as a trigger for particle deposition.

The high level of deposition control originates from immobilization of the enzyme onto the desired support. The enzyme-functionalized support is then immersed into a precursor solution. Respective enzymatic reactions thus occur only in direct proximity to the support surface, which induces controlled deposition of the particles. The high practicability on the other hand derives from the execution procedure. The entire support is simply immersed two times, first into the enzyme solution and then into the protein dispersion.

As a model system to obtain protein structures on the nanometer scale, the system casein/chymosin is utilized. Caseins are a group of proteins that make up the major protein content of milk. They have a long materials tradition as well as high potential for future applications.^{21–25} In an aqueous environment, the different caseins self-organize and form a complex aggregation structure, the casein micelle.^{26–29} The aspartic protease chymosin is able to specifically cleave the stabilizing hydrophilic parts of the protein micelle, which results in drastically changed solubility.³⁰ Application of this cleavage reaction in EMA leads to destabilized micelles in direct proximity to the support, resulting in immediate deposition of the individual protein. The process is tunable to achieve a wide variety of deposition patterns, depending on the nature of enzyme immobilization.^{18–20} Though it was possible to get nanoscaled layer thicknesses, the lateral dimensions have been on the (sub)micrometer scale.

To obtain genuine, three-dimensional nanostructures, a preceding step to prepare defined enzyme patterns is required. To sustain easy applicability and convenient execution of the overall process, pre patterning of the support with functional groups, applicable as enzyme binding sites, is the method of choice. Such a support can simply be immersed into the enzyme solution for immobilization, and afterward into the protein dispersion for particle deposition (Figure 1).

EXPERIMENTAL SECTION

Materials. Polystyrene spheres (CV < 2%, 2% (w/v)) were obtained from Microparticles Inc. and were used as received. Casein from bovine milk, chymosin, and hemoglobin were purchased from Sigma-Aldrich (Germany). (3-Glycidioxypropyl)trimethoxysilane

(GLYMO) was purchased from ABCR (Germany) and used without further purification. All other chemicals were received from local suppliers and used without further purification.

Patterning of Supports via Nanosphere Lithography. Prior to the patterning of the support surface by nanosphere lithography, silicon (100) wafers with native SiO₂ were cleaned in an oxygen/argon plasma (Oxford Instruments PlasmaLab 80 plus) with 2 sccm O₂ and 8 sccm Ar at 75 mTorr with 50 W RF power for 5 min, resulting in a hydrophilization of the surface. A monolayer of polystyrene (PS) spheres was then deposited from aqueous suspension onto the Si/SiO₂ surfaces. This is achieved by the doctor blade technique for which a droplet of the nanosphere suspension is drawn across the hydrophilic surface by a hydrophobic blade. In particular, a 40 μL droplet of the suspension was deposited on the surface, which was annealed to 26 °C, in an air atmosphere of 50% relative humidity. By this, hexagonally close-packed PS nanosphere masks were formed. The sphere masks were then modified by an oxygen/argon plasma under the same conditions as those used for the surface cleaning. The plasma treatment leads to a shrinking of the sphere diameter as PS is partially removed. The amount of removed material determines the final diameter of the shrunk spheres and can be adjusted by a variation of the plasma exposure time. In this work, larger PS spheres with an initial diameter of 618 nm were deposited on the support surface and shrunk in the plasma for 5 min to a diameter of approximately 380 nm, while 220 nm PS spheres were shrunk for 1.5 min to 160 nm. The modified monolayers of shrunk spheres were then used as shadow masks in nanosphere lithography. To this end, platinum was sputter deposited onto the sample, i.e., onto the shrunk spheres and the bare support surface between the shrunk spheres. Sputter deposition was performed in an “ISI PS-2” coating unit for 60 s at 1.2 kV and 20 μA under an argon atmosphere at 0.1 Torr. The PS spheres were subsequently dissolved by THF in an ultrasonic bath, resulting in a Pt thin film with free Si/SiO₂ substrate areas at prior sphere positions, which are accessible for enzyme immobilization.

Covalent Immobilization of Chymosin via GLYMO. Functionalization of the accessible native oxide layer of silicon wafer was achieved with GLYMO. To this, the support was immersed into a mixture of EtOH/H₂O 80:20 (w/w) with a siloxane concentration of 10% (w/w) and 1% (w/w) triethylamine. The mixture was stirred at low rounds for 2 h at 20 °C. After this, it was allowed to stand unstirred for another 10 min. Functionalized supports were then rinsed multiple times with EtOH and DI water to remove nonspecifically adsorbed GLYMO. The supports were subsequently cured for 1 h at 110 °C, rinsed with additional EtOH and DI water, and dried.

The following immobilization of chymosin was performed with 100 mL of a 1 M phosphate buffer at pH 7.0. Six mg of the freshly made enzyme formulation (62% solid enzyme content) was added to the buffer. This immobilization process was performed at 20 °C with gentle stirring. Enzyme coupling was monitored via activity tests as described in previous publications.^{13,17} Immobilization reaction was stopped after 96 h, and enzyme functionalized supports were washed with copious amounts of DI water to remove noncovalently bound chymosin and dried.

Deposition of Casein with Immobilized Chymosin. The supports with covalently immobilized chymosin on the specific

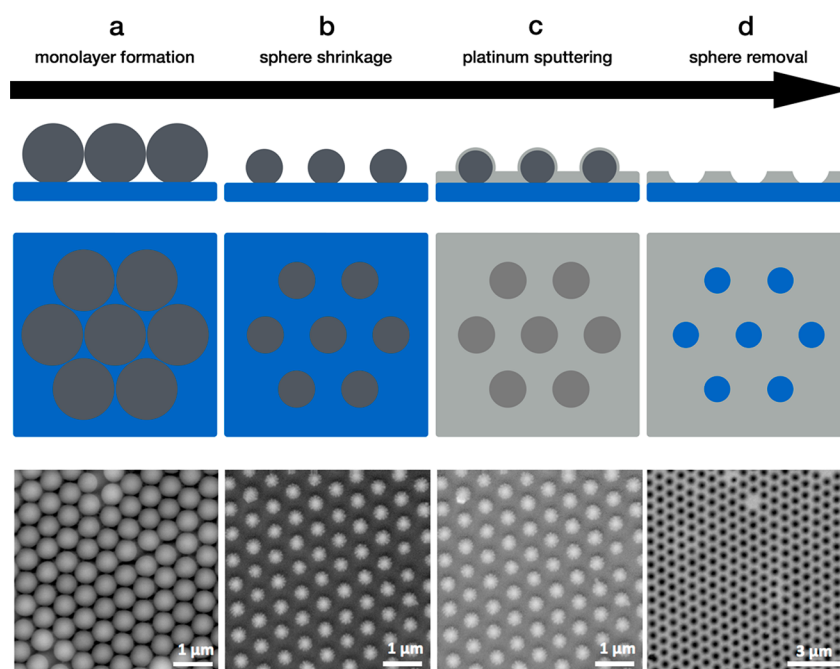


Figure 2. SEM images and respective model sketches for each step of nanosphere lithography. SiO₂ areas are shown in blue color. (a) Self-assembled hexagonally close-packed PS sphere monolayer; (b) shrunk spheres after plasma treatment; (c) sputtering with Pt; (d) subsequent removal of PS spheres yields antidot structured Pt film with free SiO₂ dots.

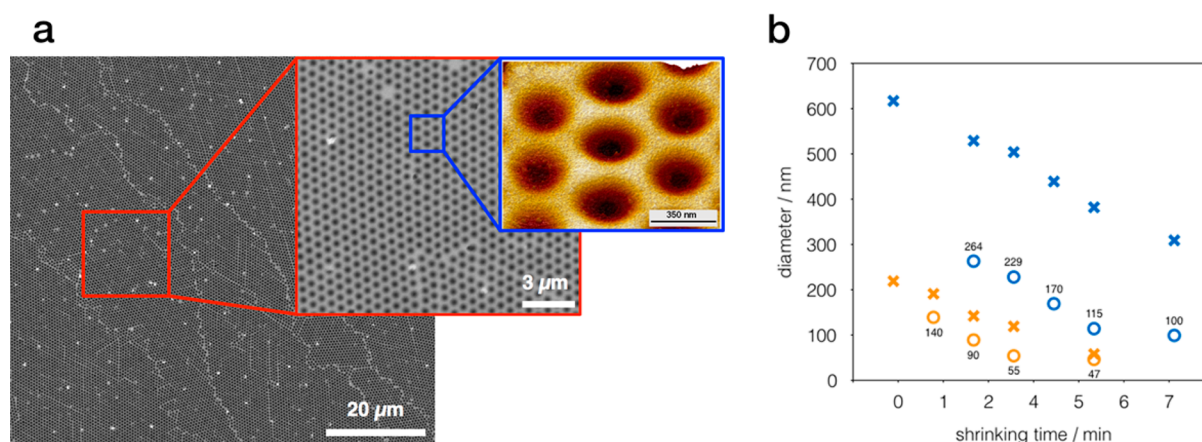


Figure 3. (a) SEM images of a representative section (100 μm²) and magnification showing uniformity of the antidot distribution over the entire support with defects <1%. The AFM picture of a single hexagon shows the decreasing Pt-layer thickness. (b) Variation of diameters of PS spheres (×) and resulting SiO₂ antidots (○) depending on time in plasma. Two examples with initial sphere diameters of 618 nm (blue) and 220 nm (orange) are shown.

patterns were immersed in a casein dispersion ($c = 1 \text{ g/L}$) at 40 °C, and remained there for 2 h. The dispersion was acidified to a pH of 3, due to the activity maximum of chymosin being at pH 3.0–4.0.³¹ After cleavage and deposition of casein micelles, the supports were rinsed twice with DI water, to remove noncleaved casein, and dried subsequently.

Characterization of Immobilized Chymosin and Obtained Casein Structures. Characterization of all stages, including supports after pre patterning, after enzyme immobilization, and after casein deposition, was performed by X-ray photoelectron spectroscopy (XPS), contact angle measurements, scanning electron microscopy (SEM), and atomic force microscopy (AFM). XPS measurements were performed with an Omicron “ESCA+” system at an energy of 50 eV for survey spectra and 25 eV for element spectra. The C 1s peak (BE = 285 eV) was used as an internal reference for calibration in all obtained spectra. Contact angle measurements of water drops were performed using a “Contact Angle Measuring System G10” from

Krüss. Contact angles were determined 1 s after placement of the drop on the support. The presented contact angles are always average values from three individual measurements. SEM images were obtained using a Jeol “JSM-6300F” scanning electron microscope at an acceleration voltage of 5 kV. For AFM imaging, a “Veeco Dimension Icon” system from Bruker was used. Measurements were conducted in PeakForce QNM mode at a constant peak force of 5 nN.

RESULTS AND DISCUSSION

Pre patterning of Support. As no biopolymers are involved in the pre patterning step, every state-of-the-art nanostructuring method is applicable. As an especially cost-effective and easy-to-apply example for patterning of surfaces on the nanometer scale, which is also suitable for large supports, nanosphere lithography (NSL) is utilized in this work.^{32–36}

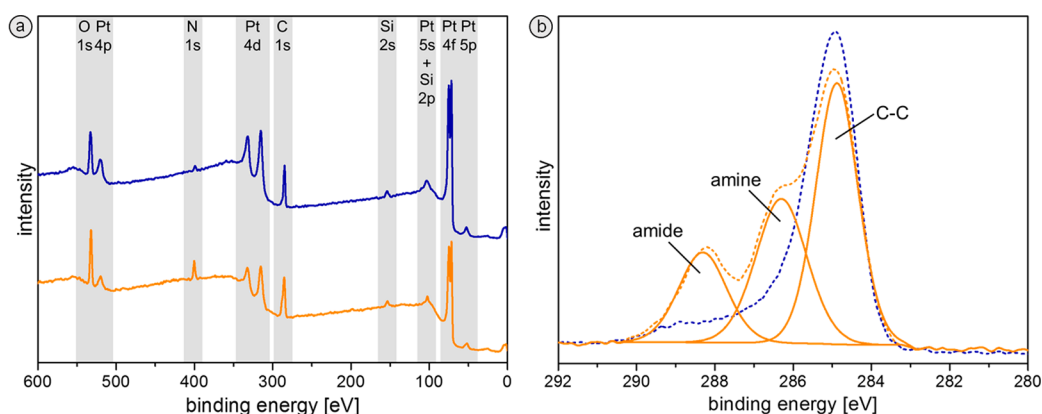


Figure 4. (a) XPS measurements of prepatterned support (blue line) before and (orange line) after enzyme immobilization. (b) XPS spectrum of the carbon C 1s peak before and after enzyme immobilization. The peak after functionalization can be deconvoluted into multiple single signals.

This technique starts with self-assembly of hexagonally close-packed monolayers of polymer spheres from colloidal suspensions. These particle monolayers act as a shadow mask for support patterning by NSL.^{32,33} A wide variety of materials can be deposited onto the support through mask openings, formed in between neighboring spheres. For a triplet of densely packed spheres, the mask opening has a triangular shape. Additionally, modification of the mask, e.g., by thermal or plasma treatment, allows for tailoring of the mask openings and the respective deposition patterns.^{37,38}

Application of NSL for the intended purpose (Figure 2) starts with the generation of large-area monolayers of polystyrene (PS) spheres on SiO₂ surfaces (silicon wafer with native oxide layer). Via the doctor blade technique, surfaces of several cm² are easily covered with uniform sphere monolayers. The layers are then treated with an oxygen/argon plasma, which results in partial removal of polystyrene. As a result, the diameter of the spheres is reduced, while their position on the support is retained.

Next, a layer of platinum (13 nm) is deposited onto the PS dots and the uncovered Si support. The smaller PS dots act as a shadow mask during the platinum sputter deposition. Finally, removal of the PS mask by chemical dissolution creates the desired material contrast between the platinum thin film and hexagonally arranged, nanoscaled SiO₂ antidots. These antidots are used as a binding site for the immobilization of enzyme in the next step.

It should be noted that the diameter of final SiO₂ antidots is not identical to that of the shrunken PS spheres. During platinum film sputter deposition, metal atoms are deposited from different directions onto the support, and thus also underneath the spheres. This can easily be confirmed via AFM imaging (Figure 3a). The topography image shows a thicker Pt film in between dots but also a decreasing film thickness toward the dot center. Only the lowest areas, identical with the contact area between support and sphere, retain the SiO₂ surface and are suitable for enzyme immobilization. The same picture also shows the high uniformity of the antidots over a large area.

The size of the antidots and their distance to each other can be tailored: The distance is determined by the initial diameter of PS spheres, while their size is set by defined oxygen plasma treatment. Figure 3b shows exemplary parameters, resulting in enzyme binding areas of 47–264 nm.

Immobilization of the Enzyme. In the second step, chymosin is immobilized on the prepatterned supports via

epoxy groups, gained by functionalization with (3-glycidyloxypropyl)trimethoxysilane (GLYMO). Success of immobilization was verified by XPS and contact angle measurements. Survey spectra, obtained for the prepatterned and enzyme-functionalized support, show significant changes which confirm coupling of enzyme (Figure 4a). Accessibility of a native oxide layer on the prepatterned Si wafer is confirmed by the respective spectrum. The maximum of the Si 2s peak is at 153.8 eV, verifying the presence of silicon oxide species. After enzyme immobilization, increased amounts of carbon and nitrogen are detected. The determined contact angle supports these findings, as it decreases from $69.2 \pm 0.6^\circ$ (before) to $43.0 \pm 0.8^\circ$ (after immobilization), caused by coupling of hydrophilic enzyme molecules.

A detailed view on the C 1s peak before and after enzyme binding contributes additional proof for the successful enzyme attachment (Figure 4b). It becomes obvious that the carbon peak after immobilization shows a combination of different C 1s species. Deconvolution into three single peaks reveals the presence of amine and amide species at 286.3 and 288.3 eV, respectively, which originate from the enzyme peptide chains. The carbon peak from before immobilization is probably caused by adsorption of low molecular hydrocarbons during sample preparation for XPS measurements. This is supported by the absence of higher oxidized carbon species.

Addressing of Protein Particles. As a final step, immersion of enzyme-functionalized supports into a casein dispersion is performed. This results in controlled deposition of cleaved protein micelles exactly and exclusively there, where immobilized enzyme is present, i.e., in the hexagonally arranged antidots. Figure 5a shows 3D-AFM height images for all three steps of the process on the example of 170 nm antidots and side-view sketches for better understanding.

The first image again shows near ideal shape and regularity of antidots on the prepatterned support. After the enzyme immobilization step (second image), several tiny particles are observable on some of the antidots, which are identified as enzyme aggregate structures. Aggregation of chymosin during the immobilization has already been observed previously and does not reduce the enzymatic activity.¹⁷ Additionally, though not determined directly, this aggregation is most certainly only partly present. First, the immobilization conditions were chosen with special attention to minimize aggregation. Second, aggregates are only observed in some antidots and only in small parts of the respective antidots; enzyme activity is present

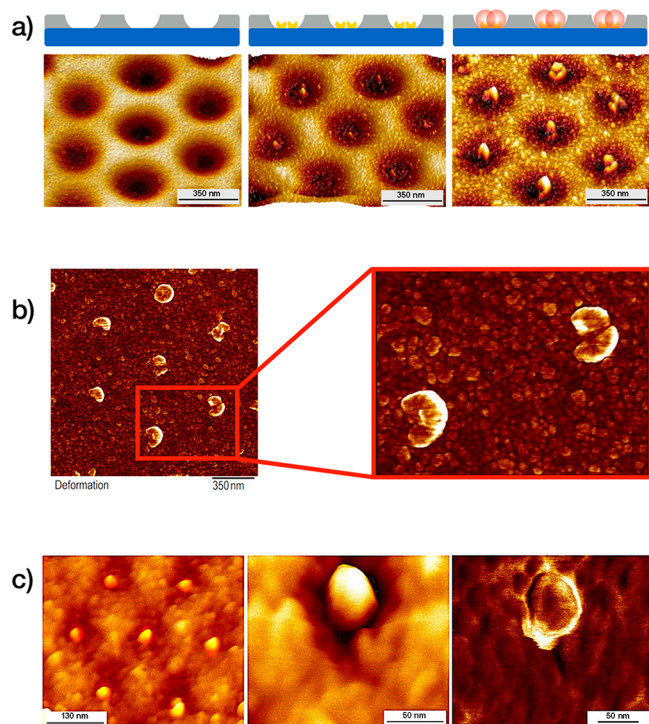


Figure 5. (a) 3D AFM height images and schematics of prepatterned support, enzyme immobilization, and protein deposition at 170 nm antidots (blue = SiO₂; gray = platinum; yellow = enzyme; red = protein). (b) AFM deformation images after casein deposition at 170 nm dots. The magnification reveals multiparticle deposition per dot. (c) AFM images of single particle deposition at 55 nm antidots: 3D height image of hexagon; 3D height image of single antidot, exhibiting one cleaved micelle; respective deformation image.

though in almost all antidots. For other, more aggregation-sensitive enzymes, the immobilization process could be adapted to exclude the effect altogether.

The third image shows the result after immersion of the support into a casein dispersion and consecutive washing procedures. This image clearly confirms site-specific deposition of cleaved protein micelles, exclusively within the designated areas. The hexagonal pattern is still recognizable after the deposition process. Immersion of control samples into a casein dispersion, which were prepatterned in the same way as described before but not functionalized with enzyme, results in no deposition at all. Self-assembly or adsorption effects can be ruled out. Thus, deposition is evidently triggered and controlled via the immobilized enzyme and takes place only in the designated areas.

In this experiment, the area of enzyme activity is 170 nm. The number mean diameter of dispersed casein micelles at the applied conditions is about 50 nm. Consequently, it is expected that several casein micelles are addressed and deposited onto each antidot. Figure 5b confirms this assumption via the AFM deformation image and a respective magnification. In this mode, the single protein particles are well distinguishable. This confirms the predicted mechanism of the process: cleaved and deposited protein micelles cover the immobilized enzyme, which leads to self-termination of the deposition process. However, the process proceeds until the whole enzyme area is covered. The AFM deformation image also provides ideal contrast between protein (soft) and support material (hard)

and confirms that protein is solely found within the hexagonal pattern.

The maximum possible specificity is the controlled addressing of single protein particles. To demonstrate this ability, a support with an antidot diameter of 55 nm is immersed into a casein dispersion. Again, the experiment yields site-specific deposition of protein particles on the antidots. This time, though, only one single particle per antidot is addressed, as shown in Figure 5c. The hexagonal pattern is perfectly retained. Magnification reveals that protein particles with diameters of 50–65 nm are deposited inside the antidots, matching the determined size of a casein micelle. At this size, a single particle covers the entire area of enzyme activity which excludes further deposition. The entire process has thereby shown its ability to completely cover any nanoscaled area of enzyme activity with a monolayer of protein particles.

Both gained structures, with 55 and 170 nm antidots, were produced three times individually, over the entire process chain, to ensure reproducibility. No significant deviation was observed in any experiment.

Identification of deposited casein micelles as cleaved particles for both systems is confirmed by washing in deionized water, which removes all noncleaved casein micelles from the surface, as previously shown.¹⁷ Further verification is delivered by determined DMT moduli: the DMT modulus of deposited casein particles is at 1.0 GPa. This is in good accordance to previous findings and differs from noncleaved casein, which has a DMT modulus of 2.4 GPa.¹⁷ Polystyrene particles, which have DMT moduli of 1.6–1.7 GPa, can also be excluded. This again demonstrates the responsibility of the enzymatic reaction for deposition.

The AFM height image (Figure 5a) additionally seemingly reveals a structuring in between the antidots, which would imply a reduced specificity. However, the AFM deformation image (Figure 5b) shows the significantly softer protein solely within the desired hexagonal patterns. It thus follows that the observed structures in the height image are not protein, but rather grounded in the platinum sputtering process, which generates a slightly rough surface topography. It is observable that this initial roughness increases with every reaction step (functionalization, immobilization, deposition). Though the reason for this is not entirely clear, unspecific protein deposition can be excluded.

The deposited casein structures also exhibit a higher flexibility, compared to conventionally processed and non-cleaved casein coatings. This is a plus, as casein is often found to be too rigid for many applications.³⁹ Additional benefits of casein coatings produced via EMA are their significantly reduced water sensitivity and enhanced stability in organic solvents.¹⁴ Moreover, sterilization processes are feasible and do not influence the material properties. This is especially important for applications, where high standards are attached to biocompatibility, e.g., in life sciences.

CONCLUSIONS

Combination of enzyme mediated autodeposition and nanosphere lithography enables an easy-to-apply and convenient approach for highly site-specific, patterned deposition of biomolecules on the nanometer scale. Hexagonal antidot patterns with variable size can specifically address protein particles. Deposition was found to continue until the entire active area is coated. After this, the reaction self-terminates. In

this fashion, single- and multiparticle addressing was equally accomplished.

The presented process offers several valuable advantages over conventional methods for nanostructuring of biomolecules. Harsh process conditions, such as organic solvents, high temperatures, or exposure to irradiation, can be averted. Moreover, the process allows for the structuring of large surfaces within a reasonable period, which is hardly obtainable via scanning probe techniques.

The prepatterning of the support does not involve biomolecules and can thus be easily performed with manifold technologies to obtain different patterns or specific nanoscaled images; it is not limited to nanosphere lithography. Enzyme immobilization as well as the actual addressing of biomolecules are then performed as easy-to-apply dip-coating processes.

Due to the inherent mechanism of the approach, deposition always stops exactly at the monolayer. It is therefore currently limited to deposition of one single layer. Different materials however might still be addressable side by side by utilization of different enzymes on different areas of the support surface.

The presented study utilized an enzymatic cleavage reaction to address protein particles. However, it has been shown previously that enzyme mediated autodeposition is transferable to other systems, like addressing of melanins.^{15,16} In principle, every process where an enzymatic reaction results in the formation of solvophobic particles should be feasible. In future work, addressing of synthetic particles will be investigated as well as other compatible biological systems. These are valuable premises for large-scale applications with potentials in biosensor technology, micro- and nanoelectronics, as well as life sciences, like implantology. For those applications, high quantity structuring of surfaces, which is provided by enzyme mediated autodeposition, is essential.

AUTHOR INFORMATION

Corresponding Author

*E-mail: oliver.strube@upb.de. Phone: +49 5251602133.

ORCID

Oliver I. Strube: [0000-0002-4357-8473](https://orcid.org/0000-0002-4357-8473)

Notes

The authors declare no competing financial interest.

ACKNOWLEDGMENTS

The authors acknowledge financial support from the European Commission within the European Fund for Regional Development Fund.

REFERENCES

- (1) Goodman, S. B.; Yao, Z.; Keeney, M.; Yang, F. The future of biologic coatings for orthopaedic implants. *Biomaterials* **2013**, *34*, 3174–3183.
- (2) Schmidmaier, G.; Wildemann, B.; Stemberger, A.; Haas, N. P.; Raschke, M. Biodegradable poly(D,L-lactide) coating of implants for continuous release of growth factors. *J. Biomed. Mater. Res.* **2001**, *58*, 449–455.
- (3) Hansen, N. M. L.; Plackett, D. Sustainable films and coatings from hemicelluloses: a review. *Biomacromolecules* **2008**, *9*, 1493–1505.
- (4) MacEwan, S. R.; Chilkoti, A. Elastin-like polypeptides: biomedical applications of tunable biopolymers. *Biopolymers* **2010**, *94*, 60–77.
- (5) Bazaka, K.; Jacob, M. V.; Crawford, R. J.; Ivanova, E. P. Plasma-assisted surface modification of organic biopolymers to prevent bacterial attachment. *Acta Biomater.* **2011**, *7*, 2015–2028.

- (6) Fotiadis, D.; Scheuring, S.; Müller, S. A.; Engel, A.; Müller, D. J. Imaging and manipulation of biological structures with the AFM. *Micron* **2002**, *33*, 385–397.

- (7) Jiang, F.; Khairy, K.; Poole, K.; Howard, J.; Müller, D. J. Creating nanoscopic collagen matrices using atomic force microscopy. *Microsc. Res. Tech.* **2004**, *64*, 435–440.

- (8) Kufer, S. K.; Puchner, E. M.; Gump, H.; Liedl, T.; Gaub, H. E. Single-molecule cut-and-paste surface assembly. *Science* **2008**, *319*, 594–596.

- (9) Morgan, H.; Pritchard, D. J.; Cooper, J. M. Photo-patterning of sensor surfaces with biomolecular structures: characterisation using AFM and fluorescence microscopy. *Biosens. Bioelectron.* **1995**, *10*, 841–846.

- (10) Graveland-Bikker, J. F.; Schaap, I. A. T.; Schmidt, C. F.; De Kruijff, C. G. Structural and mechanical study of a self-assembling protein nanotube. *Nano Lett.* **2006**, *6*, 616–621.

- (11) Rothmund, P. W. K. Folding DNA to create nanoscale shapes and patterns. *Nature* **2006**, *440*, 297–302.

- (12) Takeda, S.; et al. Lithographing of biomolecules on a substrate surface using an enzyme-immobilized AFM tip. *Nano Lett.* **2003**, *3*, 1471–1474.

- (13) Strube, O. I.; Ruediger, A. A.; Bremser, W. Enzymatically controlled material design with casein—From defined films to localized deposition of particles. *J. Biotechnol.* **2015**, *201*, 69–74.

- (14) Ruediger, A. A.; Terborg, E.; Bremser, W.; Strube, O. I. Influences on the film thickness in the enzymatic autodeposition process of casein. *Prog. Org. Coat.* **2016**, *94*, 56–61.

- (15) Strube, O. I.; Buengeler, A.; Bremser, W. Site-specific in situ synthesis of eumelanin nanoparticles by an enzymatic autodeposition-like process. *Biomacromolecules* **2015**, *16*, 1608–1613.

- (16) Strube, O. I.; Buengeler, A.; Bremser, W. Enzyme-mediated in situ synthesis and deposition of nonaggregated melanin protoparticles. *Macromol. Mater. Eng.* **2016**, *301*, 801–804.

- (17) Ruediger, A. A.; Bremser, W.; Strube, O. I. Nanoscaled biocoatings via enzyme mediated autodeposition of casein. *Macromol. Mater. Eng.* **2016**, *301*, 1181–1190.

- (18) Shindo, K.; Arima, S. Studies on the immobilized chymosin part II. *J. Fac. Agric., Hokkaido Univ.* **1979**, *59*, 284–293.

- (19) Sheldon, R. A. Enzyme immobilization: the quest for optimum performance. *Adv. Synth. Catal.* **2007**, *349*, 1289–1307.

- (20) Barbosa, O.; et al. Heterofunctional supports in enzyme immobilization: from traditional immobilization protocols to opportunities in tuning enzyme properties. *Biomacromolecules* **2013**, *14*, 2433–2462.

- (21) Audic, J.; Chaufer, B.; Daufin, G. Non-food applications of milk components and dairy co-products: a review. *Lait* **2003**, *83*, 417–438.

- (22) Silva, G. A.; Vaz, C. M.; Coutinho, O. P.; Cunha, A. M.; Reis, R. L. In vitro degradation and cytocompatibility evaluation of novel soy and sodium caseinate-based membrane biomaterials. *J. Mater. Sci.: Mater. Med.* **2003**, *14*, 1055–1066.

- (23) Vaz, C. M.; et al. Casein and soybean protein-based thermoplastics and composites as alternative biodegradable polymers for biomedical applications. *J. Biomed. Mater. Res.* **2003**, *65A*, 60–70.

- (24) Schou, M.; et al. Properties of edible sodium caseinate films and their application as food wrapping. *LWT - Food Sci. Technol.* **2005**, *38*, 605–610.

- (25) Espinoza-Castañeda, M.; et al. Casein modified gold nanoparticles for future theranostic applications. *Biosens. Bioelectron.* **2013**, *40*, 271–276.

- (26) Walstra, P. Casein sub-micelles: do they exist? *Int. Dairy J.* **1999**, *9*, 189–192.

- (27) Holt, C. Structure and stability of bovine casein micelles. *Adv. Protein Chem.* **1992**, *43*, 63–151.

- (28) Horne, D. S. Casein micelle structure: models and muddles. *Curr. Opin. Colloid Interface Sci.* **2006**, *11*, 148–153.

- (29) De Kruijff, C. G.; Huppertz, T.; Urban, V. S.; Petukhov, A. V. Casein micelles and their internal structure. *Adv. Colloid Interface Sci.* **2012**, *171–172*, 36–52.

- (30) Ruettimann, K. W.; Ladisch, M. R. Casein micelles: structure, properties and enzymatic coagulation. *Enzyme Microb. Technol.* **1987**, *9*, 578–589.
- (31) Mezina, M. N.; et al. Isolation of milk-clotting enzyme from transgenic sheep milk and its comparison with calf chymosin. *Biochemistry (Moscow)* **2001**, *66*, 378–383.
- (32) Deckman, H. W.; Dunsmuir, J. H. Natural lithography. *Appl. Phys. Lett.* **1982**, *41*, 377–379.
- (33) Hulteen, J. C.; Van Duyne, R. P. Nanosphere lithography: a materials general fabrication process for periodic particle array surfaces. *J. Vac. Sci. Technol., A* **1995**, *13*, 1553–1558.
- (34) Ye, X.; Qi, L. Recent advances in fabrication of monolayer colloidal crystals and their inverse replicas. *Sci. China: Chem.* **2014**, *57*, 58–69.
- (35) Born, P.; Blum, S.; Munoz, A.; Kraus, T. Role of the meniscus shape in large-area convective particle assembly. *Langmuir* **2011**, *27*, 8621–8633.
- (36) Dimitrov, A. S.; Nagayama, K. Continuous convective assembling of fine particles into two-dimensional arrays on solid surfaces. *Langmuir* **1996**, *12*, 1303–1311.
- (37) Riedl, T.; Strake, M.; Sievers, W.; Lindner, J. K. N. Thermal modification of nanoscale mask openings in polystyrene sphere layers. *MRS Online Proc. Libr.* **2014**, 1663, 6.
- (38) Gogel, D.; Weinl, M.; Lindner, J. K. N.; Stritzker, B. Plasma modification of nanosphere lithography masks made of polystyrene beads. *J. Optoelectron. Adv. Mater.* **2010**, *12*, 740–744.
- (39) Khwaldia, K.; Perez, C.; Banon, S.; Desobry, S.; Hardy, J. Milk proteins for edible films and coatings. *Crit. Rev. Food Sci. Nutr.* **2004**, *44*, 239–251.